Differential cross section for the $H+D_2 \rightarrow HD(v'=1,j'=2,6,10)+D$ reaction as a function of collision energy

Konrad Koszinowski,[a] Noah T. Goldberg, Jianyang Zhang, and Richard N. Zare[b]
Department of Chemistry, Stanford University, Stanford, California 94305-5080, USA

Foudhil Bouakline and Stuart C. Althorpe
Department of Chemistry, University of Cambridge, Lensfield Road, Cambridge CB2 1EW, United Kingdom

(Received 15 June 2007; accepted 18 July 2007; published online 27 September 2007)

We have measured differential cross sections (DCSs) for the HD $(v'=1,j'=2,6,10)$ products of the $H+D_2$ exchange reaction at five different collision energies in the range $1.48 \leqslant E_{coll} \leqslant 1.94$ eV. The contribution from the less energetic H atoms formed upon spin-orbit excitation of Br in the photolysis of the HBr precursor is taken into account for two collision energies, $E_{coll}=1.84$ and 1.94 eV, allowing us to disentangle the two different channels. The measured DCSs agree well with new time-dependent quantum-mechanical calculations. As the product rotational excitation increases, the DCSs shift from backward to sideward scattering, as expected. We also find that the shapes of the DCSs show only a small overall dependence on the collision energy, with a notable exception occurring for HD $(v'=1,j'=2)$, which appears bimodal at high collision energies. We suggest that this feature results from both direct recoil and indirect scattering from the conical intersection. © *2007 American Institute of Physics*. [DOI: 10.1063/1.2771157]

I. INTRODUCTION

The hydrogen exchange reaction and its isotopic variants constitute the simplest neutral bimolecular reaction. As such, they continue to be of crucial importance for molecular reaction dynamics: If we cannot achieve a complete understanding of this simplest system, we can even less expect to attain it for more complex cases and thus for almost all other chemical reactions.[1]

Despite the simplicity of the hydrogen exchange reaction, its dynamics depends on a number of variables: The masses of the involved isotopes, the quantum states of the reactants, and the collision energy, to list only a few. Together, these quantities span a large, multidimensional parameter space. To achieve a comprehensive understanding of the hydrogen exchange, as much as possible of this parameter space must be sampled. Although its immense size prohibits an exhaustive exploration, we can still hope to characterize important sections and identify the overriding trends in the dynamics of the hydrogen exchange reaction. To this end, it is not sufficient to sample only arbitrary points of the parameter space, but a systematic approach is needed.

Our groups have recently launched a project that seeks to determine the influence of the collision energy E_{coll} on the dynamics of the $H+D_2 \rightarrow HD(v',j')+D$ reaction. We demonstrated that the product rotational distributions for vibrational manifolds $v'=1-3$ depend strongly on the collision energy in the range $1.3 < E_{coll} < 1.9$ eV (for $v'=1$, the collision-energy dependence up to $E_{coll}=2.55$ eV was studied).[2–4] However, it remained unclear how the differential cross sections (DCSs), i.e., the angular distributions of the HD products, depend on E_{coll}. One previous study systematically investigated the dependence of the DCS of HD $(v'=3,j'=0)$ on E_{coll}, but the interpretation of the results was complicated by two factors: (i) The interference of a second, time-delayed mechanism specific to this quantum state and (ii) a narrow energy range.[5] Therefore the trends observed in that work cannot be easily generalized.

Here, we investigate the collision-energy dependence of the DCSs of product HD $(v'=1,j')$ in a joint experimental and theoretical study. To limit the experiments to a feasible number, we selected $j'=2$, 6, and 10 as representatives of low, medium, and high rotational states. These data should suffice to capture the major trends in the selected subspace of the reaction dynamics. In addition, our measurements enable us to correct for the contaminating effect of a second population of reactant hydrogen atoms present in this type of photoinitiated experiments. The photolysis of hydrogen bromide used for the generation of H atoms produces a small fraction of less energetic hydrogen atoms (concomitant with spin-orbit excited bromine atoms), which can also react with D_2 and thus obscure data analysis and interpretation. The contribution of these less energetic H atoms to the overall reaction was considered to be one of the largest sources of uncertainty in previous experiments of this type.[6,7]

II. EXPERIMENT

The apparatus employed in the present work[8] and its use for the determination of DCSs of HD reaction products[7] with the photoloc technique (photoinitiated reaction analyzed by

[a]Present address: Department Chemie und Biochemie, Ludwig-Maximilians-Universität München, Butenandtstrasse 5-13, Haus F, 81377 München, Germany.
[b]Author to whom correspondence should be addressed. Electronic mail: zare@stanford.edu

the law of cosines)[9,10] have already been described in detail. Here, we focus on those aspects specific to the present experiments.

A mixture of HBr (1%) in D_2 is supersonically expanded into a vacuum chamber through a pulsed valve operated at 10 Hz. The supersonic expansion cools the reagents and ensures that most of the D_2 molecules are not significantly rotationally excited ($j \leqslant 2$).[8] A pulse of linearly polarized UV laser light ($\Delta\tau \approx 5$ ns) intercepts the molecular beam at right angles and photolyzes HBr yielding atomic hydrogen and ground-state bromine, Eq. (1a). In a second reaction channel, spin-orbit-excited bromine is formed, Eq. (1b).

$$\mathrm{HBr} + h\nu \rightarrow \mathrm{H} + \mathrm{Br}(^2P_{3/2}) \tag{1a}$$

$$\rightarrow \mathrm{H} + \mathrm{Br}^*(^2P_{1/2}). \tag{1b}$$

Because the energy required for spin-orbit excitation is no longer available for the translational excitation of the hydrogen atom, reaction (1b) produces less energetic H atoms and is thus referred to as the slow channel, in contrast to the fast channel, reaction (1a). The spin-orbit excitation energy, $\Delta E_{SO} = 0.45$ eV,[11] translates into $\Delta E_{coll} = 0.36$ eV for the $H + D_2$ reaction. For the range of photolysis wavelengths sampled in the present work ($200.0 \leqslant \lambda \leqslant 220.8$ nm), the branching fraction of the slow channel is $\Gamma \approx 0.16$.[8,12] The fast and slow channels also differ in their anisotropies,[8,12] a fact that under favorable conditions could be exploited for their distinction.[7]

The H atoms generated by photolysis react with D_2 and form HD (v',j') products, which are state-selectively probed by [2+1] resonance-enhanced multiphoton ionization (REMPI) on the Q branch of the $E,F\ ^1\Sigma_g^+ - X\ ^1\Sigma_g^+$ (0,1) band.[13] The HD^+ ions are formed in the ionization region of a Wiley-McLaren time-of-flight mass spectrometer and are accelerated toward a fast, position-sensitive delay-line detector.

The nascent HD molecules move with speeds of $v \approx 10^3 - 10^4$ m/s, which result in Doppler broadening of the resonant absorption frequencies. While Doppler broadening can be overcome by using two counterpropagating UV laser pulses for the REMPI detection,[7] we chose to use only one pulse ($\Delta\tau \approx 5$ ns) for most of the present work and scan its wavelength over the Doppler profile. Because the speeds of product HD molecules formed under the current experimental conditions are moderate (compared to the speeds of the reactant H atoms) the potential signal-to-noise ratio enhancement achievable by Doppler-free spectroscopy is limited,[14] and the alignment of a third laser beam would require additional efforts. In cases where the probe laser beam could be used for photolysis at the desired wavelength ($j'=2$ at 1.73 eV and $j'=6$ at 1.69 eV), two-color Doppler-free REMPI as described in Ref. 7 was performed as well. The resulting data showed enhanced signal-to-noise ratios but otherwise were very similar to the data for $E_{coll} = 1.72$ eV acquired with an independent photolysis laser.

Finding the exact spatial overlap between the counterpropagating, focused photolysis and probe laser beams (nominal focal lengths: $f_{photolysis} = 60$, $f_{probe} = 50$ cm) is nontrivial. To avoid saturation and possible damage of the detector, the total laser power, the HBr concentration, and the particle density in the molecular beam must be limited, resulting in HD^+ count rates of less than one per laser shot. The optimization of such a small signal is inherently difficult. Moreover, the signal must be optimized against a nonzero background because the probe laser ($\lambda \approx 210$ nm) can also photolyze HBr. Therefore, finding the spatial overlap between the two lasers by direct optimization of the reactive HD^+ signal turned out to be impractical. Instead, we used two-color REMPI of static H_2, HD, or D_2 to eliminate the (resonant) one-laser background signal.[7] Passing the hydrogen over a hot tungsten filament produces vibrationally excited molecules and thus makes available a manifold of [2+1] REMPI lines in the range $201 \leqslant \lambda \leqslant 220$ nm, which can be used for finding the two-laser signal.

The H atoms originating from photolysis by the probe laser differ in their energy from those generated by the photolysis laser and thus form a contamination. Their contribution to the measured HD (v',j') signal can be eliminated by varying the relative timing of the two lasers every other shot. By firing the photolysis laser after the probe laser, we measure only the one-laser background. This background can then be subtracted from the signal measured with the photolysis laser preceding the probe laser by a reaction delay Δt to give the corrected two-laser signal. The measured HD (v',j'), signals show a linear dependence on Δt for $\Delta t \leqslant 15$ ns, but reach a maximum and decline for longer delays, indicating that HD products travel out of the focal volume of the probe laser before they could be ionized at these longer reaction delays.[2,4] To exclude any potential bias against fast moving HD products, all experiments were performed with $\Delta t \leqslant 15$ ns.

The ratio between the two-laser signal and the one-laser background depends on the powers of the photolysis and probe lasers. Increasing the power of the photolysis laser improves this ratio, and increasing the power of the probe laser strongly enhances the absolute count rates. On the other hand, higher laser powers also increase the amount of Br^+ and HBr^+, which because of space charge effects can distort the measured DCS.[7,15] To minimize the detrimental effect of these space charges, the energy of the laser pulses was restricted to $E_{pulse} < 200\ \mu$J for each laser beam. Under these conditions, the two-/one-laser signal ratios obtained ranged from 1.2:1 to 2.5:1. The lowest value of this range corresponds to the case of HD $(v'=1,j'=10)$ generated at $E_{coll} = 1.48$ eV and the highest to that of HD formed in the same quantum state at $E_{coll} = 1.94$ eV. This difference reflects both the UV absorption spectrum of HBr (Ref. 16) and the strong dependence of the integral reaction cross sections on the collision energy.[2]

From the measured positions and arrival times of the HD^+ ions, the three-dimensional velocity distribution of the nascent HD molecules can be reconstructed (the centers of the recorded three-dimensional images correspond to zero velocity). Because the energetics of the reaction are known, specific speeds can be directly mapped to specific scattering angles θ, and thus, the measured speed distribution can be converted to the DCS, denoted by $I(\theta)$. The presence of less

energetic hydrogen atoms formed in the slow channel, Eq. (1b), is ignored in this analysis and leads to systematic errors.

In order to ensure good reproducibility, each measurement was repeated at least three times over the course of at least two days. Several experiments were also repeated with new laser alignment after several weeks and yielded results very similar to the initial measurements. Typically, between 2000 and 6000 ions (remaining after subtraction of the one-laser background ions) were recorded (sum of all scans) for product HD formed in a specific quantum state at a specific collision energy. The data from each scan were separated into 20–37 angular bins and then summed; the standard deviations of the mean were taken as estimates for the statistical errors. The statistical noise can be reduced either by choosing larger bins, thus reducing the resolution, or by collecting and averaging more ions. If many scans containing only small numbers of events are summed, the quality of the resulting distribution appears to be somewhat diminished. Possible reasons for this behavior are slight differences in the experimental conditions between separate scans and imperfect centering of data sets with only small numbers of recorded ions. Also note that the use of [2+1] REMPI for detection imposes a fundamental lower limit to the bin width because the ~ 160 m s^{-1} recoil that the photoelectrons impart to the HD^+ ions broadens the measured speed distributions. We estimate that the total blurring in the present experiments ranges between 200 and 400 m s^{-1}; the additional blurring is caused mostly by the imperfect cooling of the reactants in the molecular beam and the finite focal volumes of the laser beams. Other factors, including the presence of two bromine isotopes in the HBr reactant, are negligible.[7,8]

III. THEORY

State-to-state DCSs for $H+D_2(v=0,j) \rightarrow HD(v',j')+D$ were calculated using the wave packet method of Ref. 17, in which a quantum wave packet, containing a spread of energies, is propagated from the initial $A+BC(H+D_2)$ to the final $AC+B(HD+D)$ arrangements of the reaction. Efficient basis sets are constructed from grids based on $A+BC$ Jacobi coordinates in the reagent approach region, and $AC+B$ coordinates in the transition-state and product exit regions. A separate wave packet propagation was carried out for each initial rotational quantum number $j=0,1,2$, for each individual projection Ω of j on the $A+BC$ approach vector, and for each value of the total angular momentum quantum number J in the range $J=0-35$. The basis set parameters used (in the notation of Ref. 17) were $\Delta R=0.11$ a.u., $\Delta r=0.09$ a.u., $N_\gamma=45$, and $\Omega_{max}=30$. These parameters were sufficient to yield state-to-state differential cross sections that were converged to better than 1% over the entire range of collision energies from 1.5 to 2.0 eV. The potential energy surface employed was the Boothroyd-Keogh-Martin-Peterson surface.[18] The effects of the geometric phase and of coupling to the first excited electronic surface were excluded from the calculations because these effects are known to be negligible over the range of collision energies considered.[19–21]

IV. RESULTS

As detailed in Sec. II, the experiments do not probe strictly state-to-state reactions because the reactant D_2 does not only populate the ground state but a mixture of rotational states j ($j \leqslant 2$). To make a direct comparison with the theoretical predictions possible, this rotational excitation of the reactant is explicitly accounted for in the quantum-mechanical calculations by the appropriate averaging of the contributing state-to-state DCSs and the result is subsequently blurred to account for the ionization recoil inherent in the REMPI detection scheme. The resulting averaged and blurred theoretical DCSs differ only slightly from the corresponding state-to-state DCSs for $j=0$ (Fig. 1).

The experimental DCSs shown in Fig. 2 are obtained without explicit consideration of the contributions of the slow channel (see Sec. II). We use the following method to assess the importance of these contributions and, thus, the systematic error originating from their neglect. The collision energies sampled include two pairs of E_{coll} (1.84/1.48 and 1.94/1.58 eV) which are chosen so that the minor (i.e., slow) channel of one experiment corresponds to the major (i.e., fast) channel of the other. The appropriately weighted speed distributions measured at the lower energies can then be subtracted from those obtained at the higher energies to correct for the contribution of the slow channel. The weighting takes into account the experimentally determined branching ratios for HBr photolysis,[8,12] the relative collision frequencies (proportional to $E_{coll}^{1/2}$), and the calculated relative reaction cross sections. Note that this procedure neglects the contributions of the slow channel in the speed distributions recorded for $E_{coll}=1.48$ and 1.58 eV; these second-order corrections are supposed to be quite small, and their neglect is thus not considered problematic. The corrected speed distributions for $E_{coll}=1.84$ and 1.94 eV are then converted to DCSs (Figs. 3 and 4).

Other sources of uncertainty include broadening of collision energies from residual internal energy in the HBr reagent[8] and imperfect translational cooling ($\Delta E_{coll} \approx 0.06$ eV).[2,4,22] These factors are not expected to affect the present results significantly, however.

V. DISCUSSION

A. Slow-channel correction

The described subtraction scheme allows us to correct for the contribution of the slow channel. The subtraction of the weighted HD ($v'=1, j'=6$ and 10) speed distributions obtained at $E_{coll}=1.84/1.48$ (Fig. 3, left) and 1.94/1.58 eV (Fig. 4, left) has no significant effect, that is, the neglect of the slow channel is justified for these quantum states. In contrast, the subtraction significantly shifts the maxima of the speed distributions for $j'=2$ and thus reveals substantial contributions of the slow channel at slow HD speeds.

A comparison between the raw and corrected DCSs for $E_{coll}=1.84$ (Fig. 3, right) and 1.94 eV (Fig. 4, right) shows that the corrections for HD ($v'=1, j'=6$ and 10) are very small and can be safely neglected, as already expected from the analysis of the speed distributions. Again, the situation is different for the case of $j'=2$, where the subtraction shifts

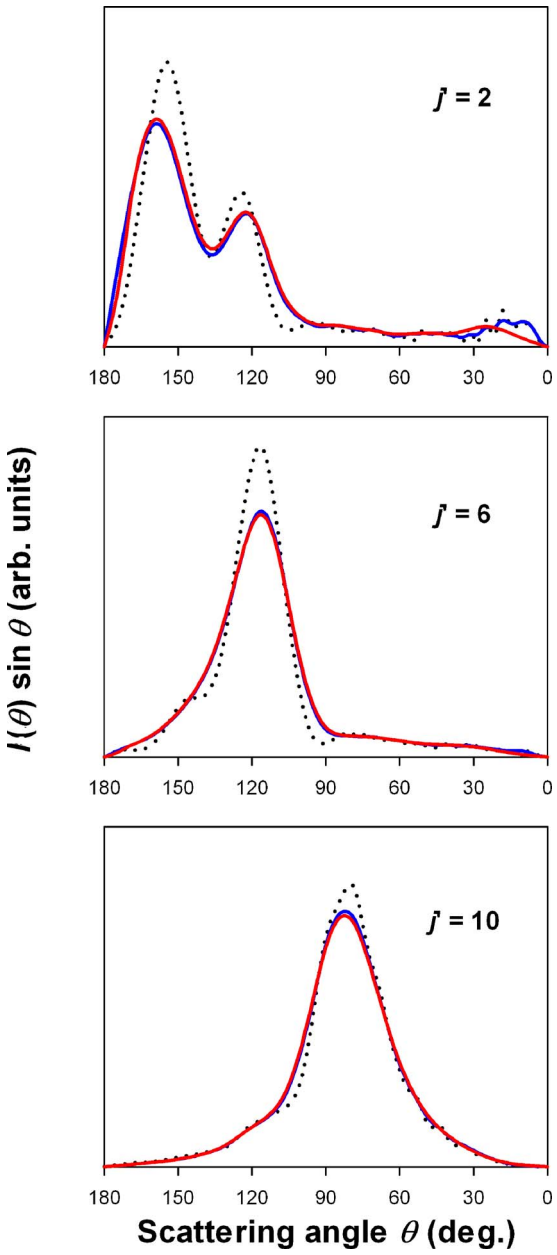

FIG. 1. (Color online) Normalized differential cross sections $I(\theta)$ of product HD $(v'=1,j')$ formed at a collision energy $E_{coll}=1.72$ eV calculated for reactant D_2 without (black dots) and with (blue lines) rotational excitation, and with rotational excitation and blurred by the ionization recoil (red lines) (see text for details). The effect of the blurring is hardly visible. The scattering angle θ is defined so that 0° corresponds to forward scattering relative to the incident H-atom direction. $I(\theta)$ is weighted by sin θ to ensure correct integration in spherical coordinates.

the maximum toward smaller scattering angles while the width of the peak is not affected. This difference between $j'=2$ on the one hand and $j'=6$ and 10 on the other hand reflects the relative populations of the j' states involved at the different energies: While the low effective collision energy of the slow channel gives rise to HD products formed in lower rotational states, the higher energy of the fast channel leads to the preferential population of higher rotational states.[2] Thus, the magnitude of the correction term is largest for low j', as is clearly visible in Figs. 3 and 4. Because the correlation between E_{coll} and rotational excitation of the product also holds for HD $(v'=2$ and 3),[3,4] this j' dependence of the correction procedure is expected to be quite general. The presented procedure solves a long-standing problem concerning the relative contributions from the slow and fast channels at a given photolysis wavelength.

B. Comparison between experiment and theory

Unlike previous studies,[5–7] the present work explicitly takes into account the effect of residual rotational excitation in reactant D_2 and thus eliminates a source of systematic error. The rotational excitation somewhat broadens the features in the DCSs but hardly changes the position of the maxima (Fig. 1). Thus, its neglect in previous studies appears largely justified. A similar conclusion was reached in work focusing on integral cross sections.[3,4] The effect of the subsequent blurring by the ionization recoil is even smaller and can be only noticed for features at small scattering angles.

Overall, experiment and theory show good agreement (Fig. 2). In several cases, such as for $j'=6$ at $E_{coll}=1.58$, 1.72, and 1.94 eV, the agreement between measured and predicted DCSs is essentially quantitative. In other cases, the agreement is not quite as good, and particularly for $j'=10$ at $E_{coll}=1.84$ eV, a significant deviation between experimental and theoretical DCSs occurs. This deviation cannot originate from the neglect of the slow-channel correction for the experimental data in Fig. 2, because the effect of this correction is insignificant for $j'=6$ and 10, as demonstrated above. The peaks of the calculated DCSs for $j'=10$ remain at nearly the same angle in the range $1.72 \leqslant E_{coll} \leqslant 1.94$ eV, whereas the maximum of the measured DCS for $E_{coll}=1.84$ eV is shifted toward larger scattering angles in comparison to those for $E_{coll}=1.72$ and 1.94 eV. Such a nonmonotonic behavior of the measured DCSs is surprising and might point to problems in the experimental conditions for this data set. In line with this assessment, the corresponding raw images show a poorer symmetry than for other experiments. However, the mistrusted experimental DCS was reproducible as reflected by the small statistical error and the close agreement of two series of measurements performed several weeks apart (Fig. 5). We also note that the observed peak in the measured DCS does not show any anomalous broadening that might be indicative of space charge distortion; space charge effects form a notorious problem in this type of experiments and special care was taken to minimize them (see Sec. II). The fact that the peak in the measured DCS is apparently shifted toward larger scattering angles also contradicts the signatures of space charge effects that we have previously observed: The electrical field of positive space charges should impart an additional acceleration to the HD^+ ions, which would then appear at too high speeds and, thus, too small angles. Hence, we do not find any obvious explanation for the deviating DCS measured for $j'=10$ at $E_{coll}=1.84$ eV.

The previous study on integral cross sections found an overall good, but not quantitative agreement between experiment and theory; the quantum-mechanically calculated rotational distributions were systematically colder than those observed in experiment.[2] It remained unclear whether these small yet distinctive deviations resulted from errors in ex-

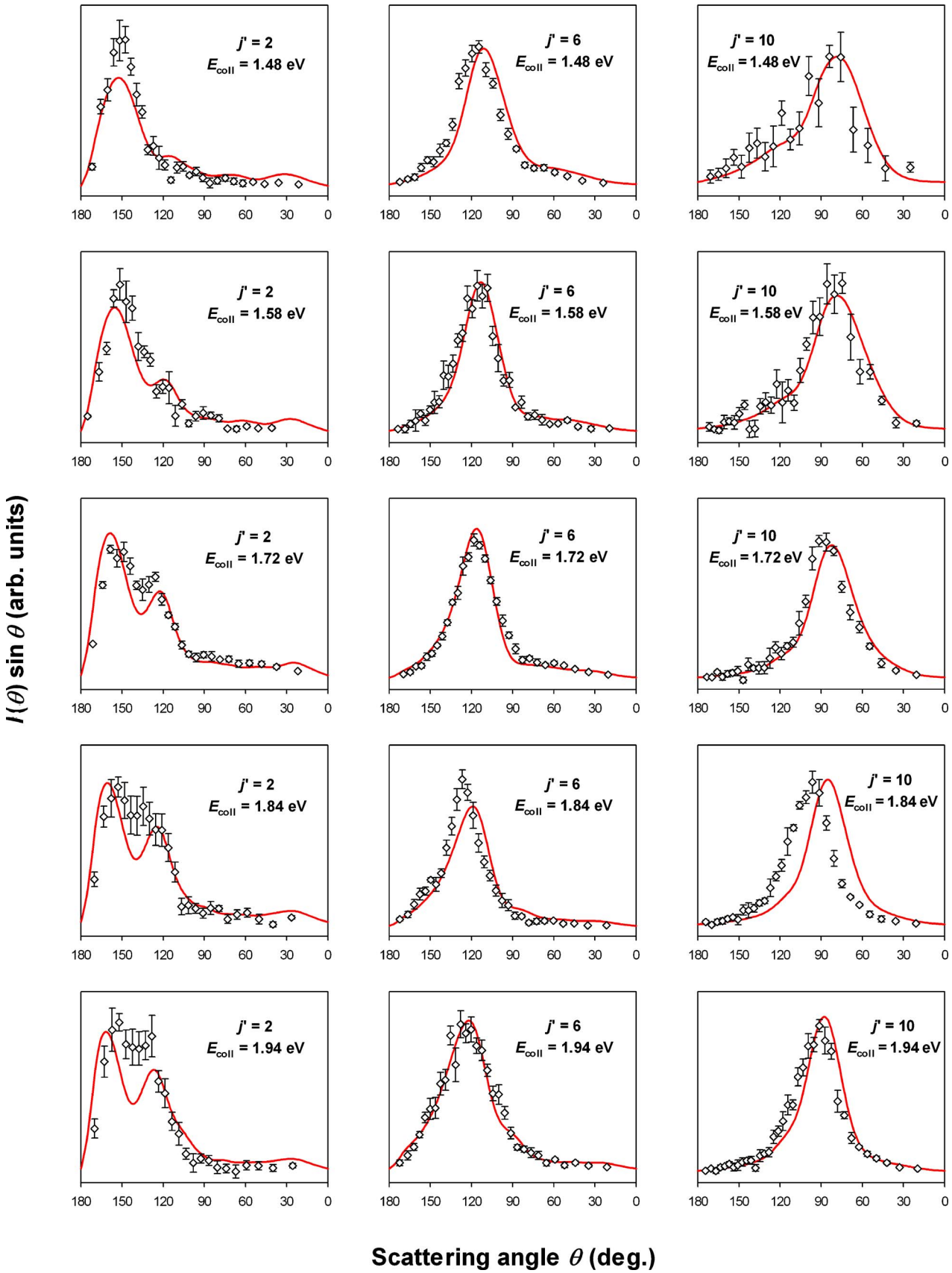

FIG. 2. (Color online) Normalized measured (diamonds) and calculated (red lines) differential cross sections $I(\theta)$ of product HD ($v'=1, j'$) formed at different collision energies E_{coll} and weighted by sin θ. The scattering angle θ is defined so that 0° corresponds to forward scattering relative to the incident H-atom direction. Statistical error bars represent one standard deviation. The experimental data for $j'=2$ and 6 that are compared to calculations for $E_{coll}=1.72$ eV were measured under Doppler-free conditions and therefore sampled slightly different collision energies ($E_{coll}=1.73$ and 1.69 eV, respectively) (see Sec. II for details). The theoretical data take into account both the rotational excitation of the reactant D_2 and the blurring caused by the ionization recoil in the REMPI detection process.

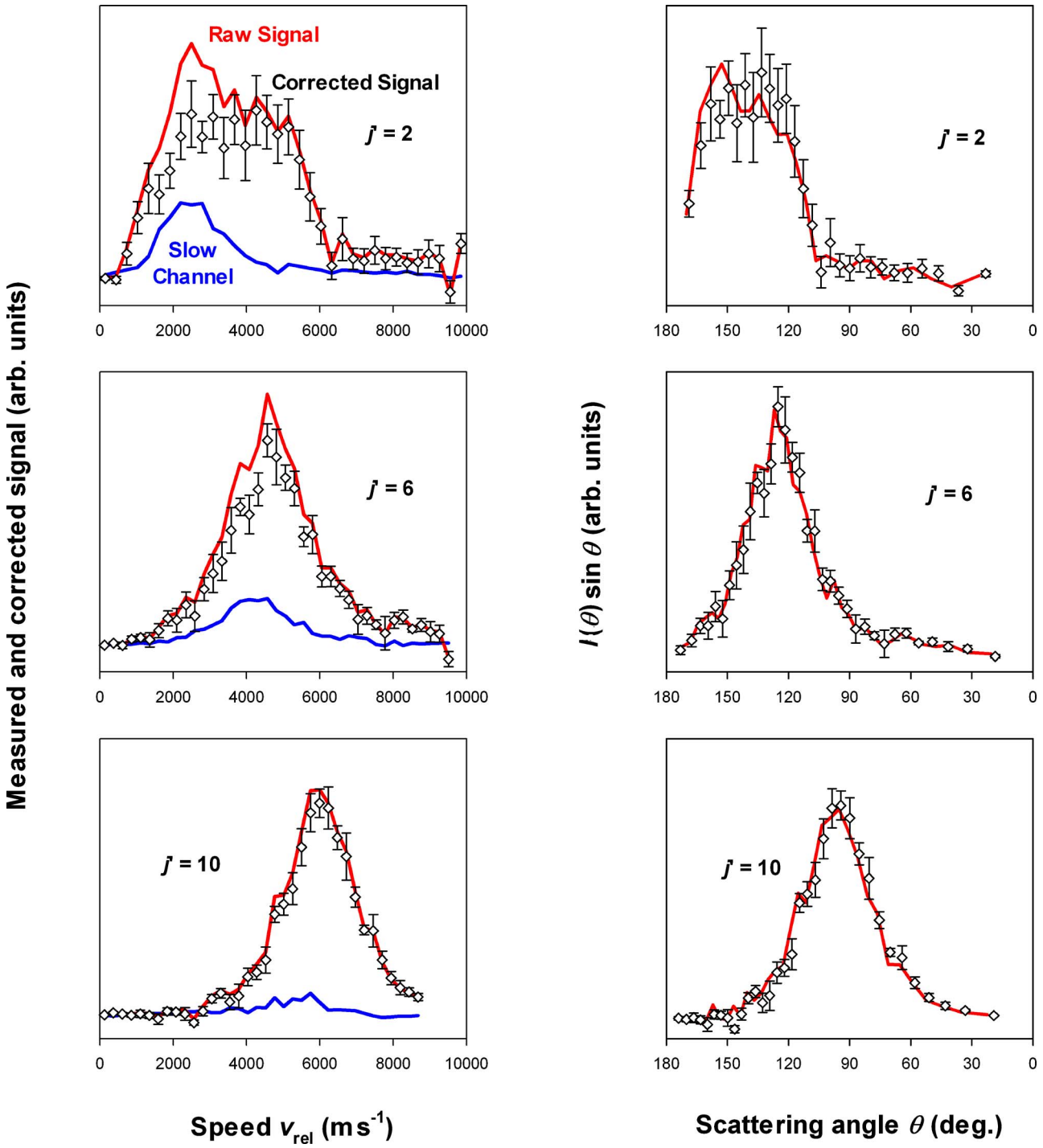

FIG. 3. (Color online) Correction for the contribution of the slow channel for product HD $(v'=1,j')$ formed at a collision energy $E_{coll}=1.84$ eV. Left: Corrected speed distributions (diamonds, error bars represent one standard deviation) obtained by subtraction of the weighted slow-channel contributions (blue lines) from the raw signals (red lines). Right: The corresponding corrected (diamonds) and raw differential cross sections $I(\theta)$ weighted by sin θ (red lines). $\theta=0°$ corresponds to forward scattering relative to the incident H-atom direction.

periment or theory (or both).[2] In light of these previous findings, it is not surprising that experiment and theory fall short of quantitative agreement in the present work because the differential cross sections are more difficult to obtain and represent a more sensitive probe of the reaction dynamics. Given that noticeable differences between experiment and theory were already evident in the relative rotational distributions, it might even be argued that the agreement found for the DCSs surpasses expectations.

C. DCS as functions of E_{coll} and j'

The DCSs of product HD $(v'=1,j')$ formed at $E_{coll}=1.48$ eV exhibit a marked dependence on the rotational state j'. While the DCS for $j'=2$ peaks at $\theta\approx150°$, the maximum for $j'=6$ lies at $\theta\approx110°$ and that for $j'=10$ at $\theta\approx80°$ (Fig. 2). For the higher collision energies investigated, very similar trends from backward to sideward scattering emerge when going from $j'=2$ to $j'=10$. Previous studies for

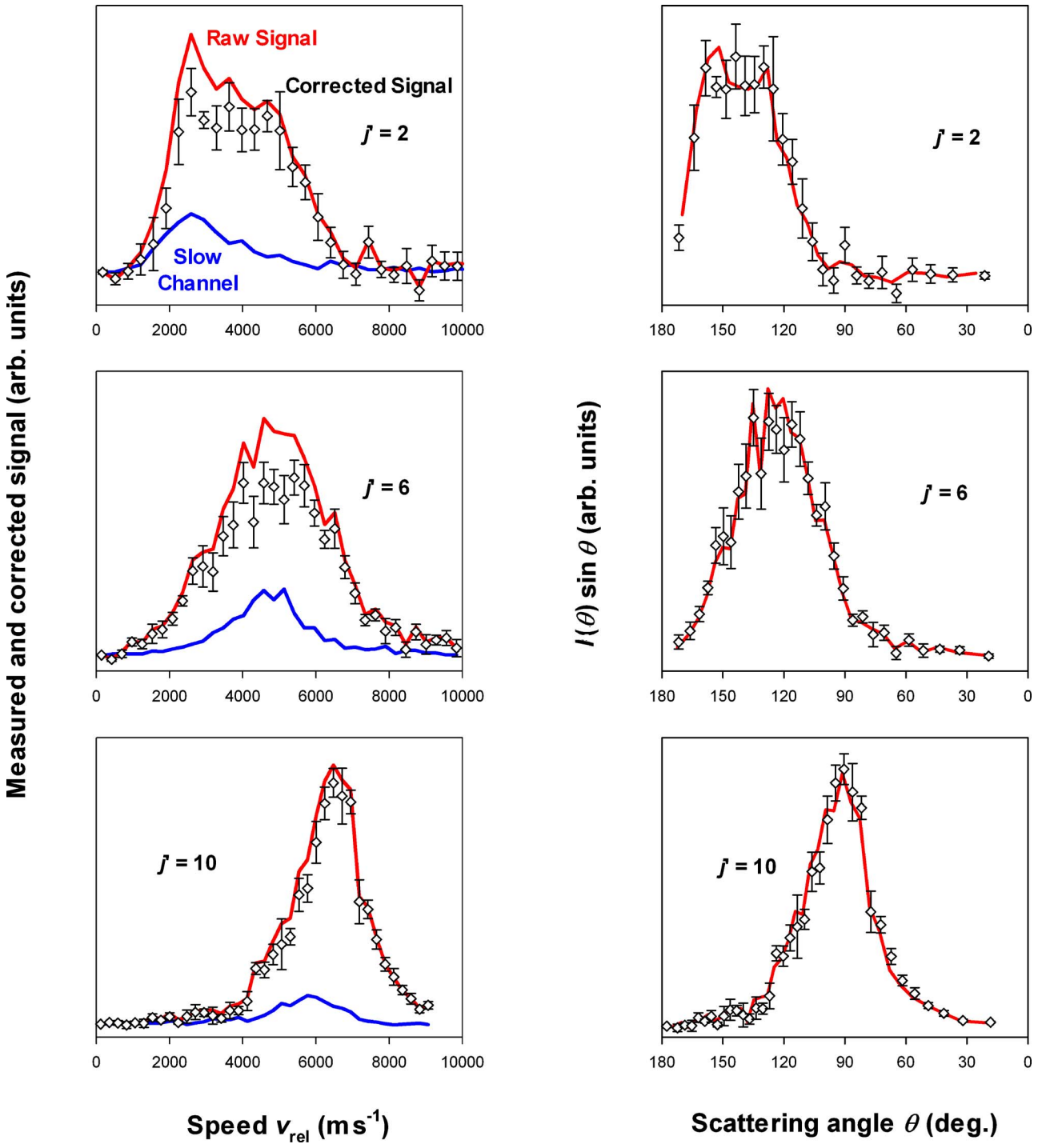

FIG. 4. (Color online) Correction for the contribution of the slow channel for product HD ($v'=1$,j') formed at a collision energy $E_{coll}=1.94$ eV. For details, see Fig. 3.

various HD vibrational manifolds and different collision energies have found an analogous j' dependence for the DCSs of the H+D$_2$ exchange reaction, which thus constitutes quite a general trend.[6,7,23–26]

Our data further allow us to assess the collision-energy dependence of the DCS for a specific rovibrational product state. This dependence is best visualized in so-called E-θ plots (Fig. 6). Unlike the calculated DCSs shown in Fig. 2, Fig. 6 presents the data for the ideal state-to-state reactions of ground-state D$_2$ without blurring by the ionization recoil. Note that these E-θ plots take into account the collision-energy dependence of the integral cross sections, in contrast to the normalized data of Fig. 2. The quantum-mechanical calculations predict a moderate decrease of the integral cross sections for $j'=2$ and 6 over the sampled range of E_{coll} but a steep increase for $j'=10$ (Fig. 6). This difference simply reflects the fact that the rotational distributions shift to higher j' states as functions of E_{coll}. This collision-energy dependence of the *integral* cross sections is well established[2] and therefore not of special interest in the present context. Instead, we focus on changes of the *shapes* of the DCSs.

The graphs for $j'=6$ and 10 are dominated by single

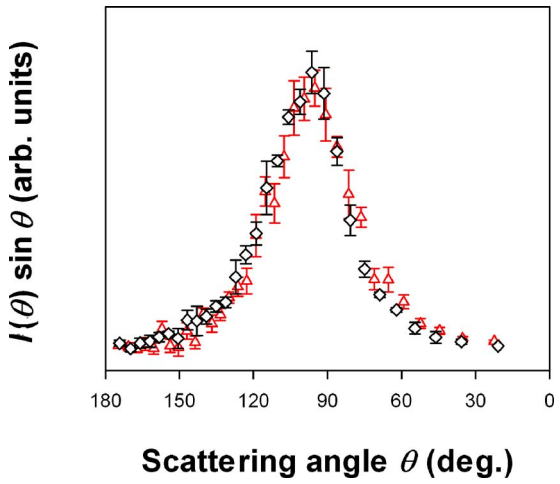

FIG. 5. (Color online) Two independent measurements of the differential cross section $I(\theta)$ of product HD ($v'=1, j'=10$) formed at a collision energy $E_{coll}=1.84$ eV and weighted by sin θ. $\theta=0°$ corresponds to forward scattering relative to the incident H-atom direction.

peaks and only for the highest collision energies sampled, a small second feature appears for $j'=6$ at $\theta \approx 95°$. In contrast, the DCS for $j'=2$ displays a second, strongly energy-dependent maximum (and a small additional third maximum at high E_{coll}). Obviously, the emergence of this side maximum does not reflect a general trend but rather represents a feature specific to this rotational state, which will therefore be discussed separately in the next section. Apart from this exception, the shapes of the DCSs change little as functions of E_{coll}. The peak for $j'=10$ somewhat narrows with increasing E_{coll}. This trend is also evident from the experimental DCSs (Fig. 2), although the analysis is hampered by the rather poor signal-to-noise ratios of the measurements at $E_{coll}=1.48$ and 1.58 eV. The worse signal-to-noise ratio obtained for $j'=10$ in comparison to $j'=2$ and 6 simply reflects the smaller relative population of the high rotational states at these collision energies.

A subtle trend common to the DCSs of all three product rotational states is a shift of the (main) maxima toward larger scattering angles for higher E_{coll}. This shift amounts to only $\approx 10°$, but despite this small value it is discernible in the experimental data as well. The low sensitivity of the DCSs for HD ($v'=1, j'=$const) to E_{coll} thus contrasts the strong j' dependence of the DCSs at constant E_{coll}.

D. Special behavior of $j'=2$

Among the DCSs determined in the present study, the second maximum in the DCSs for $j'=2$ exhibits a unique strong energy dependence and thus deserves particular attention. While this second feature at $\theta \approx 125°$ is very prominent in the calculated DCSs, it is less so in the measured DCSs. Although the measured DCSs at $E_{coll}=1.84$ and 1.94 eV in Fig. 2 appear bimodal, the separation of the two maxima does not survive the slow-channel correction (Figs. 3 and 4). Importantly, however, this correction does not change the widths of the peaks for $E_{coll}=1.84$ and 1.94 eV, which are significantly broader than those for the lower energies and also agree well with the theoretical predictions. The experiments thus essentially confirm the theoretical predictions, but the experimental data lack the resolution necessary for the distinction of both maxima. The experimental situation is likely aggravated by the relatively poor signal-to-noise ratios

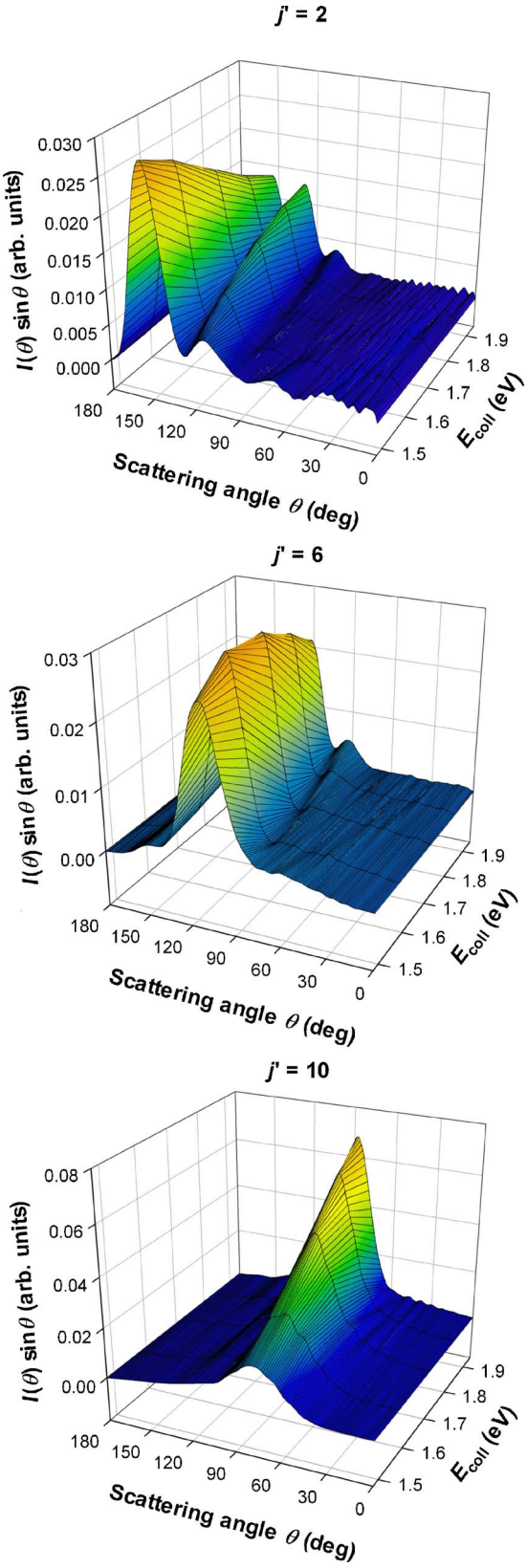

FIG. 6. (Color online) E-θ plot showing the collision-energy dependence of the calculated differential cross sections $I(\theta)$ of product HD ($v'=1, j'$) weighted by sin θ. $\theta=0°$ corresponds to forward scattering relative to the incident H-atom direction.

resulting from the low population of $j'=2$ at these energies.[2] The slow-channel subtraction procedure further increases the statistical uncertainties.

To explain the origin of the second feature in the DCS, we refer to a recent paper by Greaves *et al.*,[27] which examined quasiclassical trajectory and quantum calculations of the DCS for HD $(v'=0,j'=0)$ at $E_{coll}=1.85$ eV. This work found that, at such high collision energies, the familiar direct recoil mechanism produces mainly vibrationally excited HD products, and is unable to produce HD $(v'=0,j'=0)$. Instead, there are at least two indirect mechanisms responsible, which involve the H atom striking first the steep potential gradient that surrounds the conical intersection. These mechanisms scatter mainly into low j', and are also found in the $v'=1$ cross sections, where they compete with the direct recoil mechanism. Hence the emergence of the second feature in the $j'=2$ DCS is almost certainly a result of these indirect reaction mechanisms. A similar second maximum at $\theta \approx 130°$ also occurs in the DCS of HD $(v'=1,j'=1)$ formed at $E_{coll}=1.7$ eV.[7] Reference 27 showed that the new mechanisms can be explained largely by classical arguments. Indeed, a similar double-peak DCS for $j'=1$ was observed in earlier quasiclassical trajectory calculations.[6] The bimodal structure of the DCS for $j'=1$ is, however, less pronounced in the classical calculations, suggesting that it results from quantum interference between the recoil and the indirect mechanisms. At this stage, it is not possible to assign in detail which of the two indirect mechanisms identified in Ref. 27 is responsible for the second feature in the $j'=2$ DCS. Additional quasiclassical trajectory calculations will be needed to gain more insight about this dynamical signature characteristic of HD $(v'=1)$ products formed in low rotational states.

VI. CONCLUSIONS AND OUTLOOK

We have presented a systematic study on the collision-energy dependence of the $H+D_2 \rightarrow HD(v'=1,j')+D$ reaction. The new results amend our understanding of the dynamics of the $H+D_2$ reaction and lead to a fairly comprehensive picture of how the collision energy influences the scattering of the HD products: As demonstrated previously, an increase in E_{coll} shifts the maxima in the rotational distributions of product HD $(v'=1-3,j')$ toward higher j' states.[2–4] Our present results confirm earlier findings that this shift from lower to higher rotational states in turn is associated with a transition from backward to sideward scattering.[6,7,23–26] Moreover, we have shown that the DCS of product HD formed in a specific j' state depends only weakly on the collision energy. Thus, an increase in E_{coll} changes the scattering angle distribution mainly indirectly by its effect on the rotational distribution.

These trends have been established both by experiments and quantum-mechanical calculations. The overall agreement between the two methods is quite good but falls short of being fully quantitative. This situation resembles that encountered in our recent joint experimental and theoretical work on the integral cross sections of the title reaction.[2] Both experiment and theory also agree in the identification of a strongly energy-dependent feature in the DCS for $j'=2$. Further work is needed to elucidate the origin of this interesting behavior.

In addition, our experiments make possible to correct for the slow-channel contribution, i.e., the contribution from less energetic hydrogen atoms generated upon HBr photolysis, at $E_{coll}=1.84$ and 1.94 eV. This correction changes the corresponding DCSs only very slightly for $j'=6$ and 10, suggesting that it can be safely neglected for product HD generated in medium and high rotational states; for $j'=2$, the correction is somewhat larger and must be taken into account for a careful analysis. The slow-channel contamination is one of the major problems that have so far prevented photoloc experiments employing HI as photolytic precursor (for other problems related to the use of HI, see Ref. 15). Such experiments would be attractive because they would allow convenient access to higher collision energies $[D_0(H-I)=3.05$ vs $D_0(H-Br)=3.76$ eV$]$.[2,28] Compared to HBr, however, the use of HI as hydrogen source is complicated by the larger branching fraction for the generation of I^* at typical wavelengths $(\lambda \geqslant 210$ nm$)$.[29,30] Using the methodology applied here, the contribution of the slow channel can be easily subtracted. Moreover, the speed distributions measured in the present study cover the energy range of slow-channel HI photolysis at typical conditions. Thus, the data obtained here can be used for the slow-channel correction in future photoloc experiments employing HI as photolytic precursor.

The present study represents one of the most detailed comparisons between experiment and fully quantum-mechanical theory for the $H+H_2$ reaction system and its isotopic variants. The agreement is so close that it encourages us that theory can be relied upon for understanding the detailed behavior of this reaction over the collision-energy regime and product internal states investigated.

ACKNOWLEDGMENTS

One of the authors (K.K.) thanks the Deutsche Forschungsgemeinschaft. The Stanford team gratefully acknowledges support by the National Science Foundation under Grant No. NSF CHE 0242103. Two of the authors (F.B. and S.C.A.) acknowledge support by the UK Engineering and Physical Sciences Research Council. The first two authors contributed equally to this work.

[1] A. Teslja and J. J. Valentini, J. Chem. Phys. **125**, 132304 (2006).
[2] K. Koszinowski, N. T. Goldberg, A. E. Pomerantz, R. N. Zare, J. C. Juanes-Marcos, and S. C. Althorpe, J. Chem. Phys. **123**, 054306 (2005).
[3] F. Ausfelder, A. E. Pomerantz, R. N. Zare, S. C. Althorpe, F. J. Aoiz, L. Bañares, and J. F. Castillo, J. Chem. Phys. **120**, 3255 (2004).
[4] A. E. Pomerantz, F. Ausfelder, R. N. Zare, S. C. Althorpe, F. J. Aoiz, L. Bañares, and J. F. Castillo, J. Chem. Phys. **120**, 3244 (2004).
[5] J. D. Ayers, A. E. Pomerantz, F. Fernández-Alonso, F. Ausfelder, B. D. Bean, and R. N. Zare, J. Chem. Phys. **119**, 4662 (2003).
[6] F. Fernández-Alonso, B. D. Bean, R. N. Zare, F. J. Aoiz, L. Bañares, and J. F. Castillo, J. Chem. Phys. **115**, 4534 (2001).
[7] N. T. Goldberg, K. Koszinowski, A. E. Pomerantz, and R. N. Zare, Chem. Phys. Lett. **433**, 439 (2007).
[8] K. Koszinowski, N. T. Goldberg, A. E. Pomerantz, and R. N. Zare, J. Chem. Phys. **125**, 133503 (2006).
[9] N. E. Shafer, A. J. Orr-Ewing, W. R. Simpson, H. Xu, and R. N. Zare, Chem. Phys. Lett. **212**, 155 (1993).
[10] N. E. Shafer-Ray, A. J. Orr-Ewing, and R. N. Zare, J. Phys. Chem. **99**,

7591 (1995).
[11] C. E. Moore, *Atomic Energy Levels*, Nat. Bur. Stand. (U.S.) Circ. No. 467 (U.S. GPO, Washington, DC, 1971), Vols. 1–3.
[12] P. M. Regan, S. R. Langford, A. J. Orr-Ewing, and M. N. R. Ashfold, J. Chem. Phys. **110**, 281 (1999).
[13] E. E. Marinero, C. T. Rettner, and R. N. Zare, Phys. Rev. Lett. **48**, 1323 (1982).
[14] A. E. Pomerantz and R. N. Zare, Chem. Phys. Lett. **370**, 515 (2003).
[15] F. Fernández-Alonso, B. D. Bean, and R. N. Zare, J. Chem. Phys. **111**, 1022 (1999).
[16] B. J. Huebert and R. M. Martin, J. Phys. Chem. **72**, 3046 (1968).
[17] S. C. Althorpe, J. Chem. Phys. **114**, 1601 (2001).
[18] A. I. Boothroyd, W. J. Keogh, P. G. Martin, and M. R. Peterson, J. Chem. Phys. **104**, 7139 (1996).
[19] B. K. Kendrick, J. Chem. Phys. **118**, 10502 (2003).
[20] J. C. Juanes-Marcos, S. C. Althorpe, and E. Wrede, J. Chem. Phys. **126**, 044317 (2007).
[21] J. C. Juanes-Marcos, S. C. Althorpe, and E. Wrede, Science **309**, 1227 (2005).
[22] W. J. van der Zande, R. Zhang, R. N. Zare, K. G. McKendrick, and J. J. Valentini, J. Phys. Chem. **95**, 8205 (1991).
[23] E. Wrede and L. Schnieder, J. Chem. Phys. **107**, 786 (1997).
[24] L. Schnieder, K. Seekamp-Rahn, E. Wrede, and K. H. Welge, J. Chem. Phys. **107**, 6175 (1997).
[25] F. Fernández-Alonso, B. D. Bean, and R. N. Zare, J. Chem. Phys. **111**, 1035 (1999).
[26] F. Fernández-Alonso, B. D. Bean, and R. N. Zare, J. Chem. Phys. **111**, 2490 (1999).
[27] S. J. Greaves, D. Murdock, E. Wrede, and S. C. Althorpe, J. Chem. Phys. (unpublished).
[28] M. W. Chase, Jr., NIST-JANAF Thermochemical Tables, J. Phys. Chem. Ref. Data Monogr. **9**, 4th ed. (1998).
[29] C. A. Wight and S. R. Leone, J. Chem. Phys. **79**, 4823 (1983).
[30] D. J. Gendron and J. W. Hepburn, J. Chem. Phys. **109**, 7205 (1998).